

Wind characteristics analysis and application of control strategy for wind system based on direct power control

Bedoud Khouloud^{1,2}, Bahi Tahar², Merabet Hichem¹

¹Research Center in Industrial Technologies CRTI, Cheraga, Algeria

²Automatic Laboratory and Signals, Badji Mokhtar University, Annaba, Algeria

Article Info

Article history:

Received Jan 30, 2022

Revised Jun 4, 2022

Accepted Jun 23, 2022

Keywords:

DPC

Renewable energies

Statistical modeling

WECS

Weibull distribution

Wind energy

ABSTRACT

This study analyses yearly and seasonal wind speed data recorded over eight years using Weibull distribution function and the direct power control application of a wind chain. The wind potential evaluation was carried out based on empirical model. Results show that, during the warm months the wind speed is uniform, constant and stable. In addition, it has been found that the use of a control strategy was necessary for extracting the optimum power. For this purpose, the second part of this work presents a direct power control (DPC) technique in order to adjust the produced active and reactive powers. The application and performance evaluation of the proposed control system implemented within the d-q reference framework has been exposed and discussed. The system modeling and the control diagram are built under MATLAB software. According to simulation results, the forward power control provides almost sinusoidal input waveform current, constant switching frequency operation, unity power factor regulation and also provides powers decoupling. As shown by simulation results, the suggested control method is efficient.

This is an open access article under the [CC BY-SA](https://creativecommons.org/licenses/by-sa/4.0/) license.



Corresponding Author:

Bedoud Khouloud

Research Center in Industrial Technologies CRTI

BP 64, Cheraga, Algeria

Email: k.bedoud@crti.dz

1. INTRODUCTION

Nowadays, among renewable energy sources, wind power has become in the lead for producing electricity's. It is playing a significant role to respond the growing demand for clean and non-toxic energy thanks to its multiple advantages [1]-[3]. For these reasons, the number of installations around the world has increased considerably. Currently, because of the electricity consumption in Algeria which should be between 75 and 80 TWh in 2020 and between 130 to 150 TWh in 2030 on the other hand [3], the Algerian government provides to highlight the inexhaustible renewable resources like wind and solar energy. In this context, Algeria have plans to install 22.000 MW by 2030 to increase the electricity production to 40% by 2030 [4]-[6]. This preventive state must necessarily be achievable, because it constitutes an essential solution for Algeria so that the energy transition from the use of fossil fuels to renewable energies is ensured. Knowing that the exhaustion of fossil energies is inevitable in the near future.

Furthermore, the wind power potential is based on several parameters [7]. So, a careful study is required to install a wind power conversion system. The wind estimation and the wind power evaluation has been carried out in many countries worldwide [8]-[15]. Bamba *et al.* [14] analysed the performance of a 30 MW wind power plant in Nouakchott city, Mauritania, based on different parameters as well as the meteorological data analysis to give a good assessment of the available wind potential.

Regarding literature, Weibull model is becoming very used [16]. Hoxha *et al.* [10] has confirmed that the Weibull model is better than rayleigh model in terms of fitting wind speed variation, and this, after a statistical analysis of the wind speed in Kitka followed by a comparative study between the two models. After the study of the wind speed characteristics for Medan City, Indonesia, Suwarno *et al.* [17] has argued that the Weibull model is the better model compared to gamma and exponential distribution models.

Thus, despite that Annaba is a coastal city which has a significant wind power potential, but no work has been carried out in this context, above all, that currently Algeria is strongly involved in the field of renewable energies. For this reason that the first part of this work aims to study the wind characteristics for Annaba city using real data. To determine the yearly and seasonal power wind density and to estimate weibull scales and shapes parameters, Weibull density function (WDF) has been used.

Wind energy can be harnessed by wind energy conversion systems (WECS) which convert wind kinetic energy into electrical energy. Thanks to the remarkable advantages of variable speed WECS compared to those at a fixed speed (better energy capture and excellent quality) they are currently the most used. The remarkable development in the domain of power electronics has enabled the emergence of static converters (SC) in WECS. Due to its advantages: bidirectional energy transfer, small harmonic deformation of input currents, high power factor, lowest switching frequency and also switch voltage stress, especially attention has been given to the use of pulse width modulation PWM rectifier in WECS [18], [19]. Currently, to have a high power and sine current several SC control strategies have been developed [20]-[23]. Among these control techniques, the direct power control (DPC) has attracted attention and curiosity of many researchers thanks to its advantages [20], [24].

Aroussi *et al.* [24] has developed the maximum power point tracking MPPT control to extract optimum power for a variable speed wind power system as well as the DPC control to adjust the active and reactive power. The control technique adopted has proven a good dynamic performance and a sinusoidal waveform of currents and voltages under variable speed. Similarly, the same problem was treated by Beniss *et al.* [25] has studied a DPC control strategy and the MPPT control approach in the aim to diminish the powers errors and the selection of the suitable voltage vector. Simulation work under MATLAB/Simulink applied to 7.5 KW doubly fed induction generator DFIG wind system was carried out, demonstrating the efficiency of the used control technique. Also, in this sense, Razali *et al.* [26] has proposed a DPC control technique based on a new look-up table for three-phase grid connected to 3L-NPC. The results exposed in this work show a various performance like: low current harmonic distortion and unity power factor as well as a better dynamic response.

The present work contains of two parts, the first is based on the evaluation of wind potential per year and season of Annaba city in Algeria. The assessment and analysis of wind is important in the exploitation of wind resources. This will unquestionably allow us to have a clear forecast of wind power potential characteristics, and that our results can encourage investors to establish an energy development project in the studied site, thus taking advantage of these metrological conditions for the installation of wind turbines. Analysis of measurement results shows that the wind potential importance encourages decision makers to plan wind conversion systems installation. The recourse to energy conversion systems for the exploitation of energy sources, becomes more and more required. However, knowing that the wind speed profile is random, these wind systems require taking into account of a control system allowing to extract the maximum power whatever the real climatic data. In order to ensure a good performances and unit power factor with proper power decoupling, the second part focuses on the application of a nonlinear direct power control strategy. The optimum semiconductors switching state is selected through the switching table. Indeed, the basic idea of the switching table revolves around on dP and dQ errors variations limited by a hysteresis band, and (θ) wich is the position.

The present paper proposes in section 2, an evaluation of wind energy resources and power density. For study the wind conversion system a modelling of the whole system is carried out in section 3. After, a control based on DPC is explained and programmed under MATLAB software in section 4 and section 5, respectively. Finally, the obtained simulation results are analyzed before ending with the conclusion

2. ANALYSIS OF WIND ENERGY

Because of its several advantages, Weibull distribution is the commonly used model [17], [27] for wind speed evaluation and analysis. The mean speed is calculated as [11], [12]:

$$v_m = \frac{1}{n_i} \sum_{i=1}^n v_i \quad (1)$$

Weibull parameters: scale « c » and shape « k » can be expressed as [27], [28]:

$$k = \left(\frac{\sigma}{v_m}\right)^{-1.086} \tag{2}$$

$$c = \frac{v_m}{\gamma\left(1+\frac{1}{k}\right)} \tag{3}$$

Moreover, the c , k and v at the desired height are given as:

$$\frac{c_2}{c_1} = \left(\frac{h_2}{h_1}\right)^n \tag{4}$$

$$\frac{k_1}{k_2} = \frac{1-0,088.ln\left(\frac{h_1}{10}\right)}{1-0,088.ln\left(\frac{h_2}{10}\right)} \tag{5}$$

$$\frac{v_2}{v_1} = \left(\frac{h_2}{h_1}\right)^\alpha \tag{6}$$

Where:

$$n = \left(\frac{0,37-0,088.ln(c_1)}{1-0,088.ln\left(\frac{h_2}{10}\right)}\right) \tag{7}$$

$$\alpha = \left(\frac{0,37-0,088.ln(v_1)}{1-0,088.ln\left(\frac{h_1}{10}\right)}\right) \tag{8}$$

Wind speed data considered in this work are measured and analysed for eight (08) years (2007-2014). Figures 1(a) and (b) illustrate the monthly and yearly wind speed average at 20 m height. We notice that, 7.8973 m/s is the highest value of wind speed by month in July 2008. In addition, 4.6584 m/s is the lowest value of wind speed by month in January 2007 and February 2008.

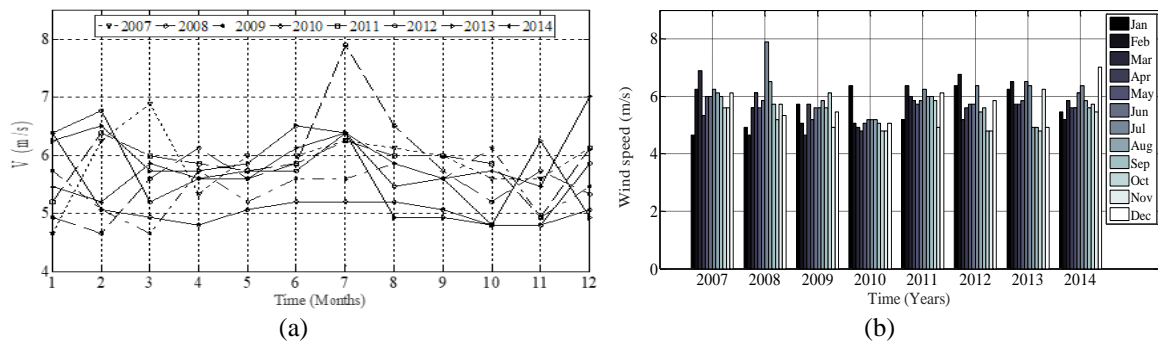


Figure 1. Wind speed by (a) months and (b) years

Figure 2 shows wind speed variation by season for eight years. The highest seasonal wind speeds is still recorded in summer. Therefore, its value during the eight years is in the range from 4.8845 m/s in Autumn 2010 to 6.7553 m/s in Spring 2008. The seasonal and yearly characteristics of wind speeds during the eight years at 20m height are recapitulated in Tables 1 and 2, respectively. The maximum average speed is 5.9638 m/s in summer, with 5.4114 m/s is the minimum average value determined in autumn.

From Figure 3 we can deduce that the scale parameter varies from 5.3379 m/s in 2010 to 6.1321 m/s in 2007. Furthermore, the shape parameter is maximum in 2007, 2009 and 2011 with a peak value of 20.3664 in 2011. Its minimal value is 4.5623 recorded in 2012. In addition, the shape parameter increases considerably in the middle of the year between May and October. Indeed, its maximal values are in spring and summer.

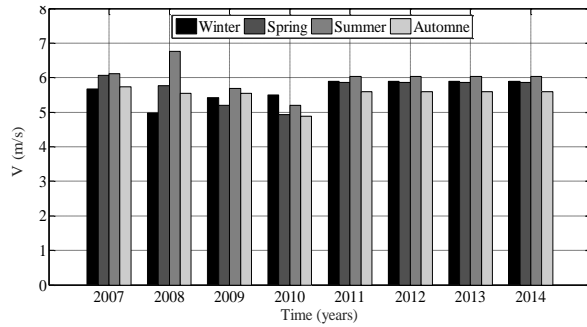


Figure 2. Seasonal wind speeds

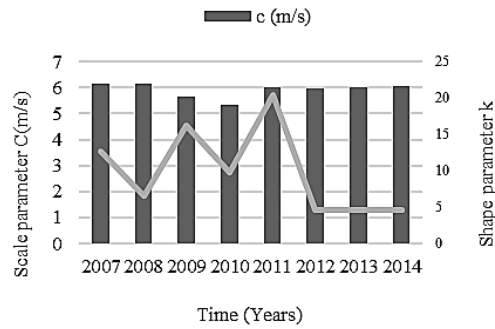


Figure 3. Yearly Weibull parameters

Table 1. Seasonal wind speed and Weibull parameters at 20 m

Period	v_{ms} m/s	k_s	c_s m/s
Winter	5,6997	10,8408	4,0086
Spring	5,5992	29,7804	5,6710
Summer	5,9638	32,9582	5,8746
Autumn	5,4114	16,9746	6,2353

Table 2. Yearly average wind speed and Weibull parameters at 20 m

Period	vm m/s	k	c m/s
2007	5,899	12,7682	6,1321
2008	5,763	06,5449	6,1299
2009	5,462	16,3110	5,6425
2010	5,128	09,8721	5,3379
2011	5,846	20,3664	6,0124
2012	5,690	04,5623	5,9563
2013	5,733	04,6174	6,0174
2014	5,824	04,6526	6,0563

3. WIND ENERGY CONVERSION SYSTEM MODEL

Conversion systems allow the conversion of the kinetic energy into electrical energy. In the case of low wind speeds the gearbox increases the rotation speed in order to ensure the required power. Do to the use of static converters, WECS presents several simple and easy control strategies compared to other systems. Figure 4 show the studied WECS.

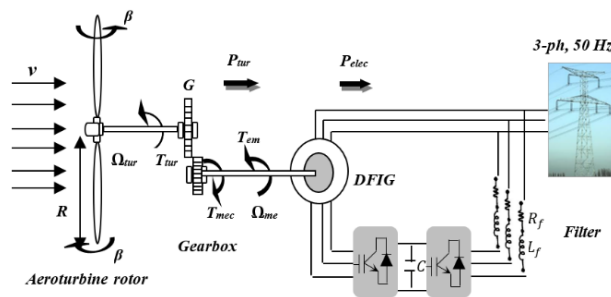


Figure 4. Schematic diagram of WECS

3.1. Mechanical part

In (9) describes the wind power [2], [29]:

$$P_v = C_p(\lambda, \beta) \cdot \frac{\rho \cdot S \cdot V^3}{2} \tag{9}$$

The power coefficient C_p can be expressed as:

$$C_p(\lambda, \beta) = 0.22 \left(\frac{116}{\lambda_i} - 0.4\beta - 5 \right) e^{-\frac{12.5}{\lambda_i}} \quad (10)$$

$$\frac{1}{\lambda_i} = \frac{1}{\lambda + 0.08\beta} - \frac{0.035}{1 + \beta^3} \quad (11)$$

$$\lambda = \frac{R \cdot \Omega_{tur}}{V} \quad (12)$$

Where: ρ is the air density and R represent rayon.

The torque is provided by the expression:

$$T_{tur} = \frac{P_{tur}}{\Omega_{tur}} = C_p(\lambda, \beta) \cdot \frac{\rho \cdot S \cdot V^3}{2} \cdot \frac{1}{\Omega_{tur}} \quad (13)$$

We can model the mechanical part by :

$$J \frac{d\Omega_{mec}}{dt} = T_{mec} - T_{em} - k_f \Omega_{mec} \quad (14)$$

When the tip speed ratio λ is optimal λ_{opt} and also C_{popt} . So, we can deduce: reference electromagnetic torque and the maximum power, determined by MPPT control [28]:

$$T_{em}^* = k_{opt} \cdot \Omega_m^2 \quad (15)$$

$$P_{max} = k_{opt} \cdot \Omega_m^3 \quad (16)$$

$$\text{With: } k_{opt} = \frac{C_{popt} \cdot \rho \cdot \pi \cdot R^5}{2 \cdot G^3 \cdot \lambda_{opt}^3}$$

3.2. Modelling of the DFIG

Considering that the grid is balanced we can write [2]:

$$\begin{bmatrix} \varphi_{ds} \\ \varphi_{qs} \\ \varphi_{dr} \\ \varphi_{qr} \end{bmatrix} = \begin{bmatrix} L_s & 0 & L_m & 0 \\ 0 & L_s & 0 & L_m \\ L_m & 0 & L_r & 0 \\ 0 & L_m & 0 & L_r \end{bmatrix} \begin{bmatrix} i_{ds} \\ i_{qs} \\ i_{dr} \\ i_{qr} \end{bmatrix} \quad (17)$$

$$\begin{bmatrix} V_{ds} \\ V_{qs} \end{bmatrix} = \begin{bmatrix} R_s & 0 \\ 0 & R_s \end{bmatrix} \begin{bmatrix} i_{ds} \\ i_{qs} \end{bmatrix} + \frac{d}{dt} \begin{bmatrix} \varphi_{ds} \\ \varphi_{qs} \end{bmatrix} + \begin{bmatrix} 0 & -\omega_e \\ \omega_e & 0 \end{bmatrix} \begin{bmatrix} \varphi_{ds} \\ \varphi_{qs} \end{bmatrix} \quad (18)$$

$$\begin{bmatrix} V_{dr} \\ V_{qr} \end{bmatrix} = \begin{bmatrix} R_r & 0 \\ 0 & R_r \end{bmatrix} \begin{bmatrix} i_{dr} \\ i_{qr} \end{bmatrix} + \frac{d}{dt} \begin{bmatrix} \varphi_{dr} \\ \varphi_{qr} \end{bmatrix} + \begin{bmatrix} 0 & -\omega_{sl} \\ \omega_{sl} & 0 \end{bmatrix} \begin{bmatrix} \varphi_{dr} \\ \varphi_{qr} \end{bmatrix} \quad (19)$$

With [2]:

$$\begin{cases} V_{ds} = \frac{d\varphi_{ds}}{dt} = 0 \\ V_{ds} = \omega_s \cdot \varphi_{ds} = V_s \end{cases} \quad (20)$$

$$T_e = 3 \frac{P}{2} L_m (i_{qs} \cdot i_{dr} - i_{ds} \cdot i_{qr}) \quad (21)$$

Where:

$\varphi_s = L_m \cdot i_{ms}$ is the stator flux and φ_r is the rotor flux;

L_s, L_m and L_r : stator, magnetizing, and rotor inductances, respectively

V_s, i_{ds} : stator voltages and currents;

V_r, i_{dr} : rotor voltages and currents;

R_r, R_s : rotor and stator resistances;

ω_e, ω_r : synchronous and rotating angular frequencies;

ω_s : synchronous angular frequency;

$\omega_{sl} = \omega_e - \omega_r$: slip frequency;

T_e : electrical torque;
 P : number of poles

3.3. Modelling of three-phase converter and PWM control

The converter mathematical modelling can be written in matrix form as:

$$\begin{bmatrix} V_{sa} \\ V_{sb} \\ V_{sc} \end{bmatrix} = R \begin{bmatrix} i_a \\ i_b \\ i_c \end{bmatrix} + L \frac{d}{dt} \begin{bmatrix} i_a \\ i_b \\ i_c \end{bmatrix} + \begin{bmatrix} V_a \\ V_b \\ V_c \end{bmatrix} \tag{22}$$

The voltages V_a , V_b and V_c are defined as [30]:

$$\begin{cases} V_a = \frac{V_{dc}}{3} (2S_a - S_b - S_c) \\ V_b = \frac{V_{dc}}{3} (S_a - 2S_b - S_c) \\ V_c = \frac{V_{dc}}{3} (S_a - S_b - 2S_c) \end{cases} \tag{23}$$

The semiconductors opening and closing of the inverter depend on the states of the control signals (S_a, S_b, S_c), respectively, as they are defined:

$$\begin{cases} S_a = \begin{cases} 1 & T_a \text{ closed and } T'_a \text{ open} \\ 0 & T_a \text{ open and } T'_a \text{ closed} \end{cases} \\ S_b = \begin{cases} 1 & T_b \text{ closed and } T'_b \text{ open} \\ 0 & T_b \text{ open and } T'_b \text{ closed} \end{cases} \\ S_c = \begin{cases} 1 & T_c \text{ closed and } T'_c \text{ open} \\ 0 & T_c \text{ open and } T'_c \text{ closed} \end{cases} \end{cases} \tag{24}$$

$$S_k = \begin{cases} +1, \overline{S_k} = -1 \\ 0, \overline{S_k} = +1 \end{cases} \tag{25}$$

Or, $k=a, b, c$.

DC-Bus equation is given by:

$$C \frac{dV_{dc}}{dt} = S_a i_a + S_b i_b + S_c i_c - S_c i_l \tag{26}$$

4. CONTROL STRATEGY DESCRIPTION

In order to calculate the semiconductors switching state for powers control, we used a hysteresis regulators. The powers variations are the inputs of the regulators. Furthermore, the basic idea of the switching table articulated on dP and dQ errors variations limited by a hysteresis band as shown in Figure 5. The DPC [20]-[23] is a nonlinear and direct control because it doesn't use any modulation technique.

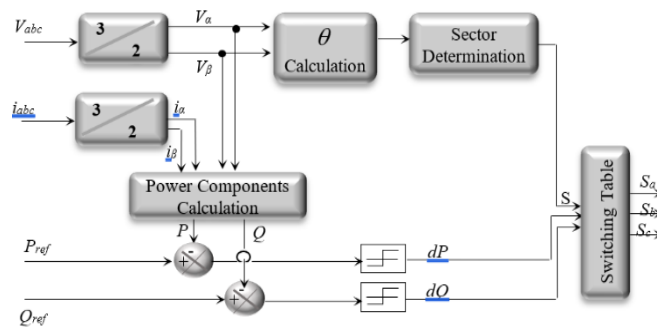


Figure 5. Inverter control block

Thus, there are eight combinations which develop at the inverter output, six vectors of active voltages

(V_i with $i=1:6$) and two vectors of zero voltages (V_0) and (V_7), as given in Table 3. The eight possible voltage vectors in the Clark plane (α, β) are shown by the polygon of Figure 6. They are expressed by the:

$$V_k = \sqrt{\frac{2}{3}} V_{dc} e^{jk\pi/3} \tag{27}$$

With, $k=1, \dots, 6$ and $V_0 = V_7 = 0$

Table 3. Switching states and output voltages

S_a	S_b	S_c	U_{ca}	U_{cb}	U_{cc}	U_{ca}	U_{cb}	V_i
0	0	0	0	0	0	0	0	V_0
0	0	1	$-\frac{V_{dc}}{3}$	$-\frac{V_{dc}}{3}$	$-\frac{2V_{dc}}{3}$	$-\frac{V_{dc}}{3}$	$-\frac{V_{dc}}{3}$	V_5
0	1	0	$-\frac{V_{dc}}{3}$	$\frac{2V_{dc}}{3}$	$-\frac{V_{dc}}{3}$	$-\frac{V_{dc}}{3}$	$\frac{\sqrt{6}}{3}$	V_3
0	1	1	$-\frac{2V_{dc}}{3}$	$\frac{V_{dc}}{3}$	$\frac{V_{dc}}{3}$	$-\frac{2}{3}V_{dc}$	$\frac{\sqrt{6}}{3}$	V_4
1	0	0	$-\frac{2V_{dc}}{3}$	$\frac{V_{dc}}{3}$	$\frac{V_{dc}}{3}$	$\frac{2}{3}V_{dc}$	0	V_1
1	0	1	$\frac{V_{dc}}{3}$	$-\frac{2V_{dc}}{3}$	$\frac{V_{dc}}{3}$	$\frac{V_{dc}}{3}$	$\frac{V_{dc}}{3}$	V_6
1	1	0	$\frac{V_{dc}}{3}$	$\frac{V_{dc}}{3}$	$-\frac{2V_{dc}}{3}$	$\frac{V_{dc}}{3}$	$\frac{\sqrt{6}}{3}$	V_2
1	1	1	0	0	0	0	0	V_7

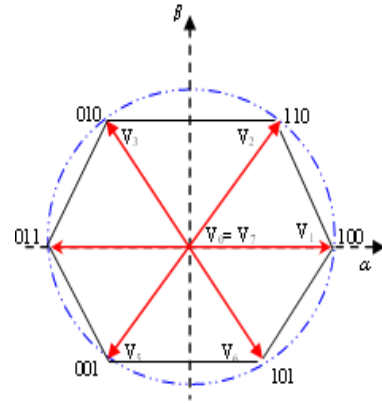


Figure 6. Switching polygon

The hysteresis controllers are at two levels for the P and Q powers where their outputs are represented by the boolean variables dP and dQ indicating, respectively, the higher or lower overruns of the following active (P) and reactive (Q) power errors according to the following logic:

$$\begin{cases} P_{ref} - P \geq h_p \Rightarrow dP = 1 \\ P_{ref} - P < h_p \Rightarrow dP = 0 \\ Q_{ref} - Q \geq h_q \Rightarrow dQ = 1 \\ Q_{ref} - Q < h_q \Rightarrow dQ = 0 \end{cases} \tag{28}$$

Where, h_p and h_q are the hysteresis bands regulators. For this purpose, in the case where the errors are greater than zero the regulator output is equal to 1 else its equal to 0. The purpose of this type of power controller is to maintain the end of the error of the active or reactive power in a hysteresis band of 2h. The hysteresis corrector output indicates if the power error must be increased ($dP=1$), ($dQ=1$) or decreased ($dP=0$), ($dQ=0$). Furthermore, V_{dc} can be regulated using PI controller as shown in Figure 7. Figure 8 presents the regulation of DC voltage with a PI controller.

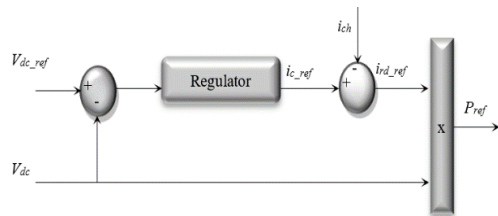


Figure 7. Calculation of the reference power

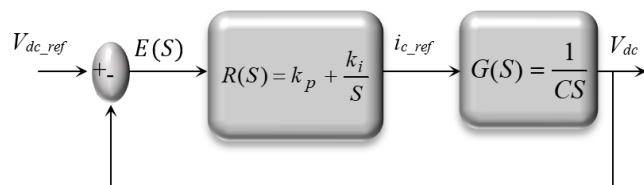


Figure 8. DC voltage regulation with a PI controller

Where, the output voltage is multiplied by the effective DC bus voltage V_{dc} to generate P_{ref} . We can write [29]:

$$\frac{V_{dc}}{V_{dc_ref}} = \frac{k_p \cdot k_i / K}{S^2 + k_p / K \cdot S + k_p \cdot k_i / K} \tag{29}$$

Where:

$$K = \frac{\sqrt{2}CV_{dc.ref}}{3V_s} \tag{30}$$

According to the in (31), the relation between V_{dc} and $V_{dc.ref}$ reveals be a second order transfer function:

$$\frac{V_{dc}}{V_{dc.ref}} = \frac{\omega_n^2}{s^2 + 2\xi\omega_n s + \omega_n} \tag{31}$$

The PI controller parameters are chosen according to the following relationships:

$$\begin{cases} k_p = 2\xi\omega_n K \\ k_i = \omega_n / 2\xi \end{cases} \tag{32}$$

The reference continued current is expressed by:

$$I_{rd.ref} = I_{c.ref} + I_{ch} \tag{33}$$

Where:

I_{ch} : reference current in the capacitor given by the regulator PI of the voltage

$I_{c.ref}$: measured load current;

$I_{rd.ref}$: reference continued current.

The product of the reference DC current with the DC voltage gives the reference active power:

$$P_{ref} = V_{dc.ref} \cdot I_{rd.ref} \tag{34}$$

We can write the active and reactive powers as:

$$\begin{cases} p_s = V_{sa} \cdot i_{sa} + V_{sb} \cdot i_{sb} + V_{sc} \cdot i_{sc} \\ Q_s = \frac{1}{\sqrt{3}}(V_{sb} - V_{sc})i_{sa} + (V_{sc} - V_{sa})i_{sb} + (V_{sa} - V_{sb})i_{sc} \end{cases} \tag{35}$$

Hence, we can estimate the voltage using the:

$$\begin{bmatrix} V_\alpha \\ V_\beta \end{bmatrix} = \frac{1}{i_\alpha^2 + i_\beta^2} \begin{bmatrix} I_\alpha & -I_\alpha \\ I_\alpha & I_\alpha \end{bmatrix} \begin{bmatrix} P_s \\ Q_s \end{bmatrix} \tag{36}$$

The reactive power reference is maintained at the desired value (generally zero to have a unit power factor). The P_{ref} is calculated by multiplication current value generated and the optimum voltage [31]. The two hysteresis controllers' outputs and the source voltage vector position are the switching table inputs. Depending to the vector angle of the reference source voltage on the axis (α), we decompose the position space into twelve sectors as shown in Figure 9. Where, it can be determined by [32]:

$$(N - 2) \frac{\pi}{6} < \theta_N < (N - 1) \frac{\pi}{6} \tag{37}$$

Where, $N=1, 2, \dots, 12$.

The sector number (N) is instantly determined by the voltage vector position given by:

$$\theta = \arctg\left(\frac{V_\beta}{V_\alpha}\right) \tag{38}$$

Table 4 presents the switching table which is the essential part in the DPC control [23]. It enables the selection of the voltage vector to allow the orientation of the active and reactive powers towards their designated values.

Table 4. Switching table

dP	dQ	θ_1	θ_2	θ_3	θ_4	θ_5	θ_6	θ_7	θ_8	θ_9	θ_{10}	θ_{11}	θ_{12}
1	1	V_6	V_7	V_1	V_0	V_2	V_7	V_3	V_0	V_4	V_7	V_5	V_0
1	0	V_7	V_7	V_0	V_0	V_7	V_7	V_0	V_0	V_7	V_7	V_0	V_0
0	1	V_6	V_1	V_1	V_2	V_2	V_3	V_3	V_4	V_4	V_5	V_5	V_6
0	0	V_1	V_2	V_2	V_3	V_3	V_4	V_4	V_5	V_5	V_6	V_6	V_1

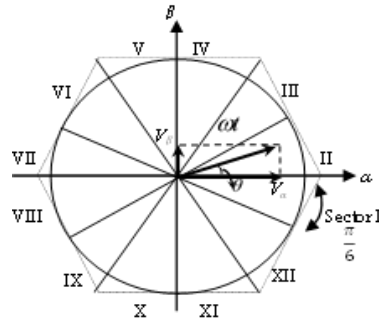


Figure 9. Position of different sectors [31]

5. RESULTS AND DISCUSSION

The whole system was carried out using MATLAB/Simulink (see Figure 10). We have considered a wind profile evolving according to the Figure 11(a) with a wind speed of 12 m.s^{-1} between $0 \leq t < 1\text{s}$ and equal to 9 m.s^{-1} between $1 < t \leq 2\text{s}$. Thus, the couple and the generator speed evolve according to the paces represented by the Figures 11(b) and 11(c), respectively. However, the electrical network voltages and currents waveform are purely sinusoidal whose figures are shown, respectively, by Figures 12(a) and 12(b) (see Appendix). Moreover, for more details, the Figures 12(c), 12(d) and 12(e) (see Appendix) present zooms or parts of these last figures.

We notice that, the amplitude of the network currents changes with the change in wind speed. And that, since we have considered a reference of the variable reactive power ($Q=0$ if $0 < t \leq 0.5\text{s}$; $Q=4 \text{ KVar}$ if $0.5 < t \leq 1\text{s}$; $Q=2 \text{ KVar}$ if $1 < t \leq 1.5\text{s}$ and $Q=0$ if $1.5 < t \leq 2\text{s}$) we note that the currents waveforms (Figure 12(c)) change in amplitude (see the circled zooms A and B). Finally, Figures 13(a)-(c), highlight the paces of: active power, reactive power and a zoom of reactive power. We can see that the reactive power follows its reference perfectly as defined above. However, at times $t=0.5 \text{ s}$ and $t=1.5 \text{ s}$, the active power keeps its reference value notwithstanding the reactive power variation. These, witnesses and valid the studied control strategy, which ensures a powers decoupling.

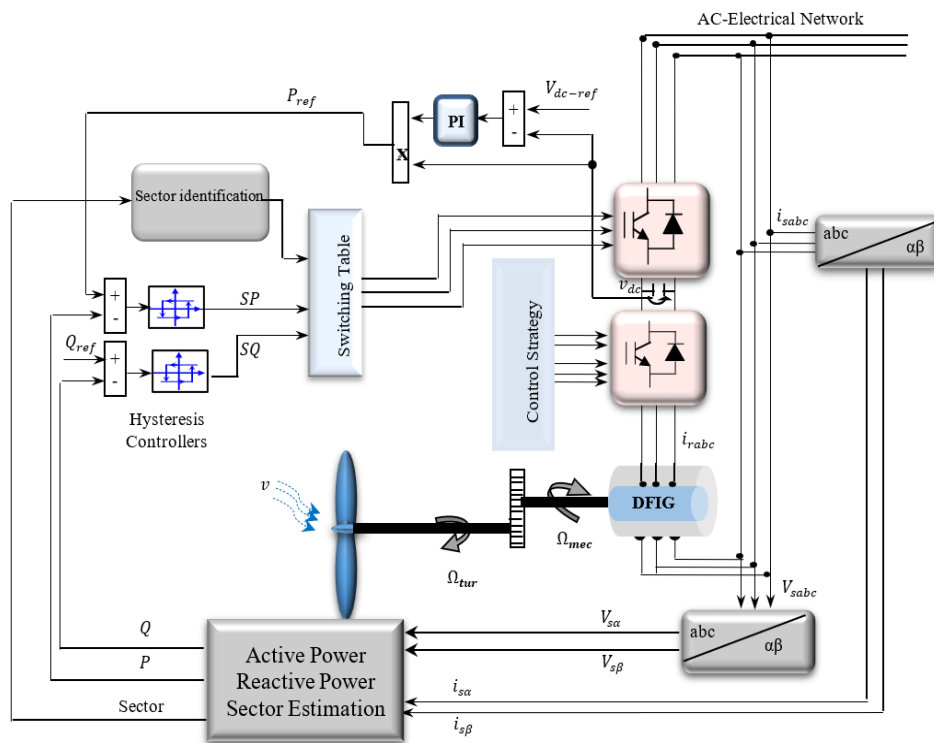


Figure 10. Schematic diagram of the proposed control algorithm

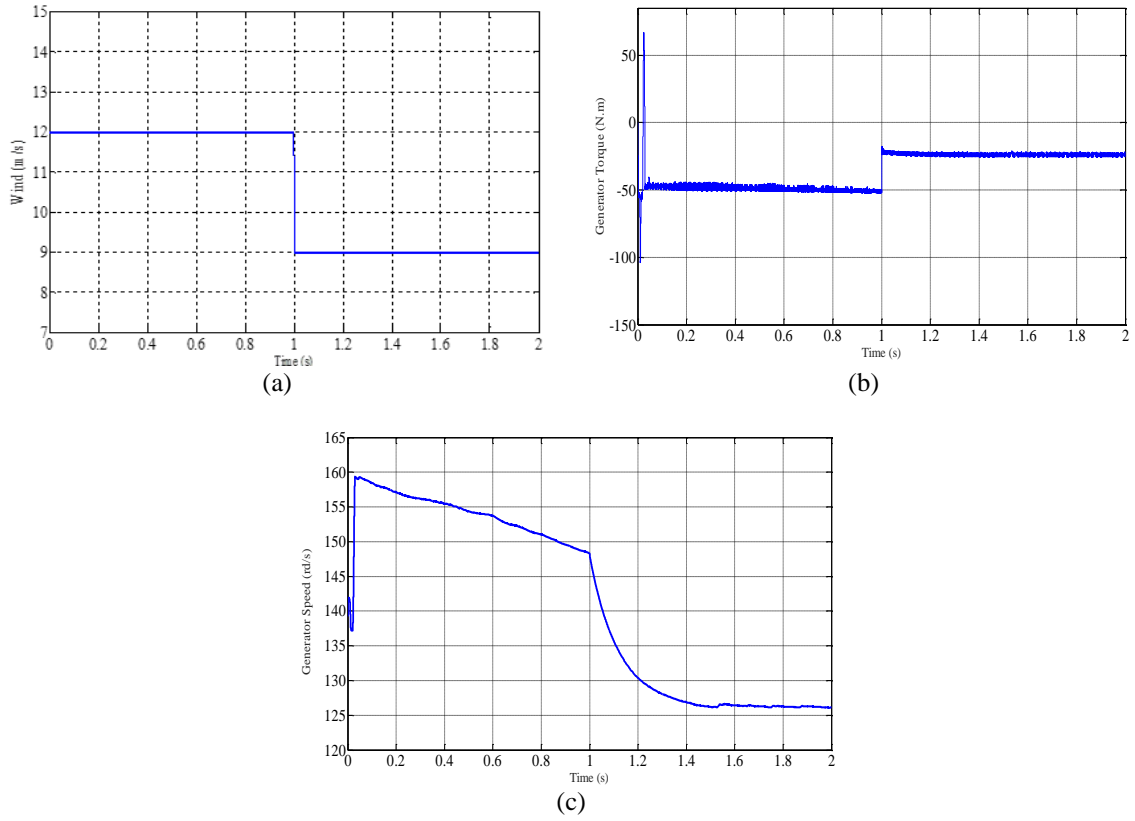


Figure 11. The simulation results for (a) wind speed, (b) torque, and (c) generator speed

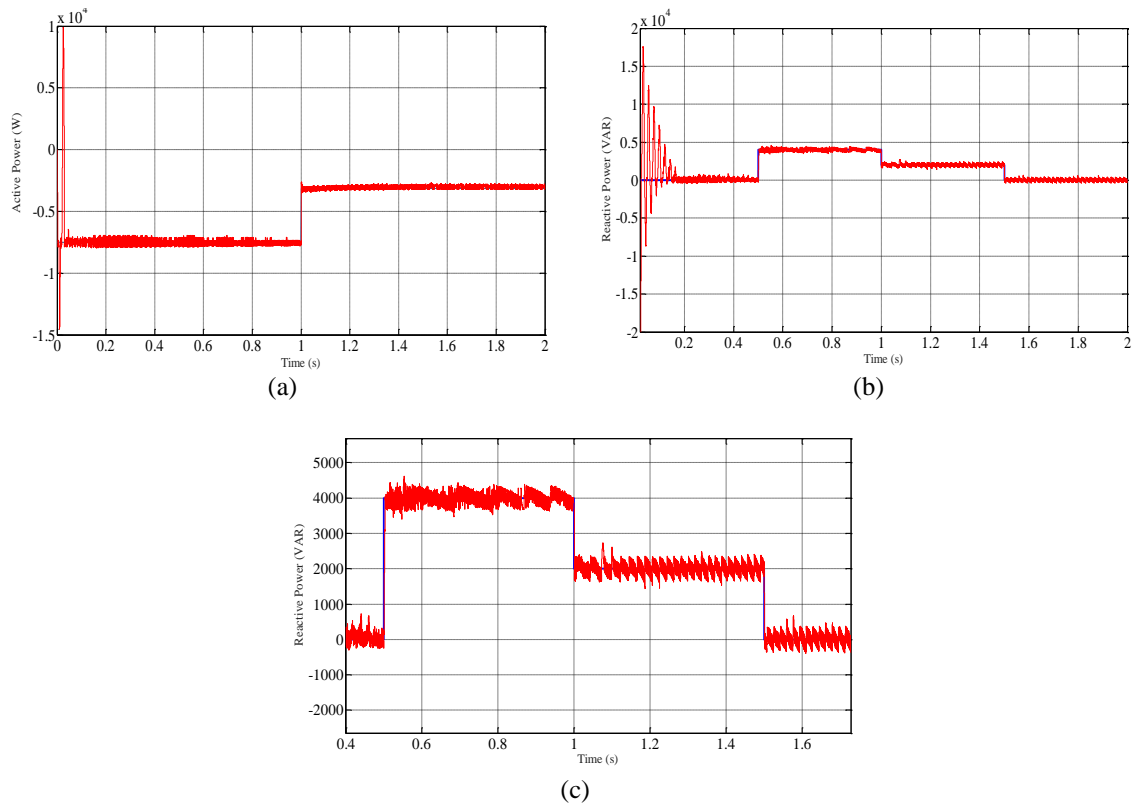


Figure 13. The power curves (a) active power, (b) reactive power, and (c) reactive power zoom

6. CONCLUSION

In this paper, an evaluation of wind potential of a site in Annaba, Algeria was carried out in prevision of wind power production chain installation. The results showed that Annaba city has a reasonably average wind farm with a peak of nearly 6.7553 m/s at 20 m altitude in Spring 2008 and 7.8973 m/s in July 2008. Based on this analysis, it should be noted that we can use the wind capacity for power production. Finally, as a coastal city, Annaba can be suggested as one of the desirable's places for the installation of wind turbines. Furthermore, the DPC control strategy has used. The simulation results of P and Q powers give very high performances in term of response time and overshoot. Furthermore, a good decoupling between the active and reactive powers was assured by the proposed control strategy thus guaranteeing a unity power factor for $0 < t \leq 0.5s$ and $1.5 < t \leq 2s$. So, this command has proven to be sufficient in such cases. However, the application of robust and intelligent commands will certainly be the subject of our future work.

APPENDIX

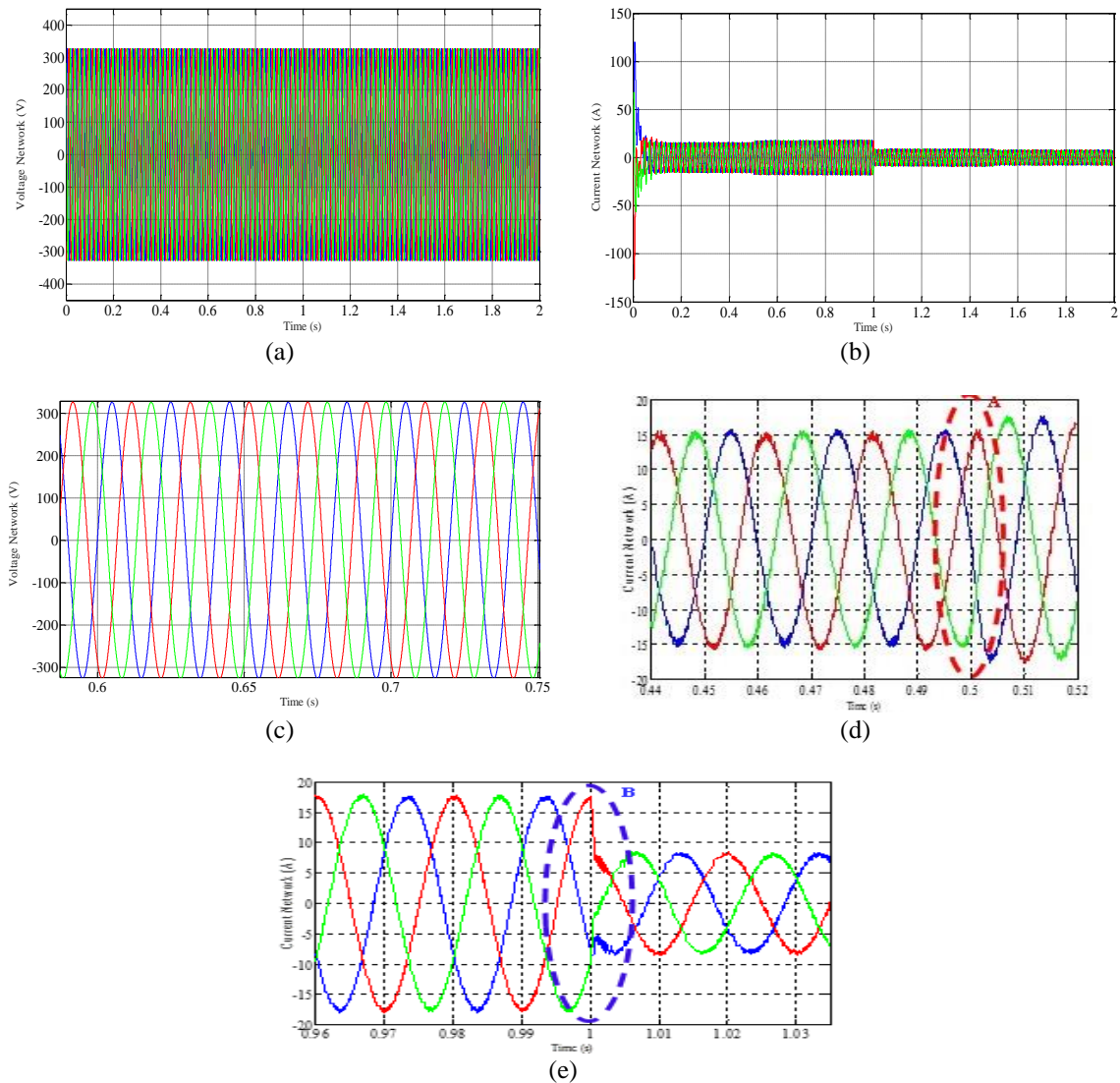


Figure 12. The simulation results for, (a) voltages network, (b) voltage zoom, (c) currents network, (d) currents zoom for $t=0.5$, and (e) currents zoom for $t=1$

REFERENCES

[1] Y. Ihdrane, C. E. Bekkali, and B. Bossoufi, "Improved Performance of DFIG-generators for Wind Turbines Variable-speed," *International Journal of Power Electronics and Drive System*, vol. 9, no. 4, pp. 1875-1890, 2018, doi: 10.11591/ijpeds.v9.i4.pp1875-1890.

- [2] K. Bedoud, A. Rhif, T. Bahi, and H. Merabet, "Study of a double fed induction generator using matrix converter: Case of wind energy conversion system," *International Journal of Hydrogen Energy*, vol. 43, no. 25, pp. 11432-11441, 2018, doi: 10.1016/j.ijhydene.2017.07.010.
- [3] Z. Abada, and M. Bouharkat, "Study of management strategy of energy resources in Algeria," *Energy Reports*, vol. 4, pp. 1-7, 2018, doi: 10.1016/j.egy.2017.09.004.
- [4] S. A. Boudghene, Z. Khiat, S. Flazi, and Y. Kitamura, "A review on the renewable energy development in Algeria: Current perspective, energy scenario and sustainability issues," *Renewable and Sustainable Energy Reviews*, vol. 16, no. 17, pp. 4445-4460, 2012, doi: 10.1016/j.rser.2012.04.031.
- [5] S. M. Boudia, A. Benmansour, N. Ghellai, M. Benmedjahed, and H. M. A. Tabet, "Temporal assessment of wind energy resource at four locations in Algerian Sahara," *Energy Conversion and Management*, vol. 76, pp. 654-664, 2013, doi: 10.1016/j.enconman.2013.07.086.
- [6] S. Diaf, and G. Notton, "Evaluation of electricity generation and energy cost of wind energy conversion systems in southern Algeria," *Renewable and Sustainable Energy Reviews*, vol. 23, pp. 379-390, 2013, doi: 10.1016/j.rser.2013.03.002.
- [7] A. S. Badawi *et al.*, "Data bank: nine numerical methods for determining the parameters of weibull for wind energy generation tested by five statistical tools," *International Journal of Power Electronics and Drive Systems*, vol. 12, no. 2, pp. 1114-1130, 2021, doi: 10.11591/ijpeds.v12.i2.pp1114-1130.
- [8] C. F. D. Andrade, F. M. N. Hely, P. A. C. Rocha, and M. E. V. D. Silva, "An efficiency comparison of numerical methods for determining weibull parameters for wind energy applications: A new approach applied to the northeast region of Brazil," *Energy Conversion and Management*, vol. 86, pp. 801-808, 2018, doi: 10.1016/j.enconman.2014.06.046.
- [9] H. Qinkai, M. Sai, W. Tianyang, and C. Fulei, "Kernel density estimation model for wind speed probability distribution with applicability to wind energy assessment in China," *Renewable and Sustainable Energy Reviews*, vol. 115, pp. 1-14, 2018, doi: 10.1016/j.rser.2019.109387.
- [10] B. Hoxha, R. Selimaj, and S. Osmanaj, "An experimental study of weibull and rayleigh distribution functions of wind speeds in kosovo," *Telecommunication Computing Electronics and Control*, vol. 16, no. 5, pp. 2451-2457, 2018, doi: 10.12928/TELKOMNIKA.v16i5.10260.
- [11] K. Azada, M. Rasul, P. Halder, and J. Sutariya, "Assessment of Wind Energy Prospect by Weibull Distribution for Prospective Wind Sites in Australia," *Energy Procedia*, vol. 160, pp. 348-355, 2019, doi: 10.1016/j.egypro.2019.02.167.
- [12] T. Aukitino, M. G. M. Khan, and A. M. Rafiuddin, "Wind energy resource assessment for Kiribati with a comparison of different methods of determining weibull parameters," *Energy Conversion and Management*, vol. 151, pp. 641-660, 2017, doi: 10.1016/j.enconman.2017.09.027.
- [13] Z. H. Hulioa, J. Wei, and S. Rehman, "Techno-Economic assessment of wind power potential of Hawke's Bay using Weibull parameter: A review," *Energy Strategy Reviews*, vol. 26, pp. 1-13, 2019, doi: 10.1016/j.esr.2019.100375.
- [14] H. Bamba, A. M. Yahya, M. Q. Taha, N. Khezam, and A. K. Mahmoud, "Performance analysis of 30 MW wind power plant in an operation mode in Nouakchott, Mauritania," *International Journal of Power Electronics and Drive System*, vol. 12, no. 1, pp. 532-541, 2021, doi: 10.11591/ijpeds.v12.i1.pp532-541.
- [15] Suwarno and Rohana, "Wind speed modeling based on measurement data to predict future wind speed with modified Rayleigh model," *International Journal of Power Electronics and Drive System (IJPEDS)*, vol. 12, no. 3, pp. 1823-1831, 2021, doi: 10.11591/ijpeds.v12.i3.pp1823-1831.
- [16] M. K. Saeed, A. Salam, A. Rehman, and S. M. Abid, "Comparison of six different methods of weibull distribution for wind power assessment: A case study for a site in the Northern region of Pakistan," *Sustainable Energy Technologies and Assessments*, vol. 36, 2019, doi: 10.1016/j.seta.2019.100541.
- [17] Suwarno, I. Yusuf, M. Irwanto, and A. Hiendro, "Analysis of wind speed characteristics using different distribution models in Medan City, Indonesia," *International Journal of Power Electronics and Drive System*, vol. 12, no. 2, pp. 1102-1113, 2021, doi: 10.11591/ijpeds.v12.i2.pp1102-1113.
- [18] N. Muangruk, and S. Nungam, "Direct Power Control of Three-phase Voltage Source Converters Using Feedback Linearization Technique," *Procedia Computer Science*, vol. 86, pp. 365-368, 2016, doi: 10.1016/j.procs.2016.05.100.
- [19] T. Shi, J. Wang, C. Zhang, and C. Xia, "Direct power control for three-level PWM rectifier based on hysteresis strategy," *Science China Technological Sciences*, vol. 55, pp. 3019-3028, 2012, doi: 10.1007/s11431-012-4999-y.
- [20] L. I. Mengdi, W. U. Xuan, S. Huang, and I. Gel, "Model predictive direct power control using optimal section selection for PWM rectifier with reduced calculation burden," *International Journal of Electrical Power & Energy Systems*, vol. 116, 2020, doi: 10.1016/j.ijepes.2019.105552.
- [21] W. Taha, A.R. Brig, and I. Boiko, "Quasi optimum PI controller tuning rules for a gridconnected three phase AC to DC PWM rectifier," *International Journal of Electrical Power & Energy Systems*, vol. 96, pp. 74-85, 2018, doi: 10.1016/j.ijepes.2017.09.027.
- [22] M. Zarif, and M. Monfared, "Step-by-step design and tuning of VOC control loops for grid connected rectifiers," *International Journal of Electrical Power & Energy Systems*, vol. 64, pp. 708-713, 2015, doi: 10.1016/j.ijepes.2014.07.078.
- [23] J. Huang, F. Guo, C. Wen, B. Yang and J. Xiao, "A Direct Power Control Strategy for AC/DC Converter Based on Best Switching State Approach," *IEEE Journal of Emerging and Selected Topics in Power Electronics*, vol. 6, no. 4, pp. 2273-2286, 2018, doi: 10.1109/JESTPE.2018.2832663.
- [24] H. A. Aroussi, E. Ziani, M. Bouderbala, and B. Bossoufi, "Enhancement of the direct power control applied to DFIG-WECS," *International Journal of Electrical and Computer Engineering*, vol. 10, no. 1, pp. 35-46, 2020, doi: 10.11591/ijece.v10i1.pp35-46.
- [25] M. A. Beniss, H. E. Moussaoui, T. Lamhamdi, and H. E. Markhi, "Performance analysis and enhancement of direct power control of DFIG based wind system," *International Journal of Power Electronics and Drive System*, vol. 12, no. 2, pp. 1034-1044, 2021, doi: 10.11591/ijpeds.v12.i2.pp1034-1044.
- [26] A. M. Razali, N. A. Yusoff, K. A. Karim, A. Jidin, and T. Sutikno, "A new switching look-up table for direct power control of grid connected 3L-NPC PWM rectifier," *International Journal of Power Electronics and Drive Systems*, vol. 12, no. 3, pp. 1413-1421, 2021, doi: 10.11591/ijpeds.v12.i3.pp1413-1421.
- [27] A. N. Celik, and M. Kolhe, "Generalized feed-forward based method for wind energy prediction," *Applied Energy*, vol. 101, pp. 582-588, 2013, doi: 10.1016/j.apenergy.2012.06.040.
- [28] A. S. A. Badawi, N. F. Hasbullah, S. H. Yusoff, Aand . Hashim, "Energy and power estimation for three different locations in Palestine," *Indonesian Journal of Electrical Engineering and Computer Science*, vol. 14, no. 3, pp. 1049-1056, 2019, doi: 10.11591/ijeecs.v14.i3.pp1049-1056.
- [29] S. Mensou, A. Essadki, I. Minka, T. Nasser, B. B. Idrissi, and L. B. Tarla, "Performance of a vector control for DFIG driven by wind turbine: real time simulation using DS1104 controller board," *International Journal of Power Electronics and Drive System*, vol. 10, no. 2, pp. 1003-1013, 2019, doi: 10.11591/ijpeds.v10.i2.pp1003-1013.

- [30] K. Bedoud, M. Ali-rachedi, T. Bahi, and R. Lakel, "Adaptive Fuzzy Gain Scheduling of PI Controller for Control of the Wind Energy Conversion Systems," *Energy Procedia*, vol. 74, pp. 211-225, 2015, doi: 10.1016/j.egypro.2015.07.580.
- [31] A. Chaoui, J. P. Gaubert, and A. Bouafia, "Direct power control switching table concept and analysis for three-phase shunt active power," *Journal Electrical Systems*, vol. 9, no. 1, pp. 52-65, 2013.
- [32] A. Chaoui, F. Krim, and J. P. Gaubert, "Power quality improvement using DPC controlled three phase shunt active filter," *Electric Power Systems Research*, vol. 80, no. 6, pp. 657-666, 2010, doi: 10.1016/j.epsr.2009.10.020.

BIOGRAPHIES OF AUTHORS



Bedoud Khoulood    is a lecturer in Research Center in Industrial Technologies, Algeria since 2011. She got the Eng degree in electronics at Baadji Mokhtar University in 2005. She became an assistant researcher in 2010, a senior researcher (B) in 2016, and a senior researcher (A) in 2018. Her current research interests include the field of power electronics and its applications such as renewable energy, control system, motor drive, nano-technology, industrial diagnosis and artificial intelligence. She has published as author or co-author several articles in the fields of renewable energies. She can be contacted at email: k.bedoud@crti.dz.



Bahi Tahar    is a professor in Electrical Engineering Department at Badji Mokhtar University, Algeria. He got the Eng, Magister and Ph.D degrees in electrical engineering at Badji Mokhtar University in 1983, 1986 and 2006, respectively. His research interests revolve around the power electronic, motor drive, wind energy, photovoltaic system. He has published as author or co-author several articles in the fields of power electronics and its applications. He can be contacted at email: tbahi@hotmail.fr.



Merabet Hichem    is a lecturer in Research Center in Industrial Technologies, Algeria since 2011. He got the Eng degree in electronics at Baadji Mokhtar University in 2006. He became an assistant researcher in 2009, a senior researcher (B) in 2016, and a senior researcher (A) in 2018. His research interests revolve around the power electronic, motor drive, wind energy, photovoltaic system, industrial diagnosis. He has published as author or co-author several articles in the fields of power electronics and its applications. He can be contacted at email: h.merabet@crti.dz.